Self-organized criticality in neural networks from activity-based rewiring

Stefan Landmann, Lorenz Baumgarten, and Stefan Bornholdt[*]
Institut für Theoretische Physik, Universität Bremen, Germany

Neural systems process information in a dynamical regime between silence and chaotic dynamics. This has lead to the *criticality hypothesis*, which suggests that neural systems reach such a state by self-organizing toward the critical point of a dynamical phase transition. Here, we study a minimal neural network model that exhibits self-organized criticality in the presence of stochastic noise using a rewiring rule which only utilizes local information. For network evolution, incoming links are added to a node or deleted, depending on the node's average activity. Based on this rewiring-rule only, the network evolves toward a critical state, showing typical power-law-distributed avalanche statistics. The observed exponents are in accord with criticality as predicted by dynamical scaling theory, as well as with the observed exponents of neural avalanches. The critical state of the model is reached autonomously without the need for parameter tuning, is independent of initial conditions, is robust under stochastic noise, and independent of details of the implementation as different variants of the model indicate. We argue that this supports the hypothesis that real neural systems may utilize such a mechanism to self-organize toward criticality, especially during early developmental stages.

I. INTRODUCTION

Neural systems, to efficiently process information, have to operate at an intermediate level of activity, avoiding both a chaotic regime as well as silence. It has long been speculated that neural systems may operate close to a dynamical phase transition that is naturally located between chaotic and ordered dynamics [1–4]. Indeed, recent experimental results support the criticality hypothesis, most prominently the so-called neuronal avalanches, specific neuronal patterns in the resting state of cortical tissue which are power-law distributed in their sizes and durations [5–9]. Studies suggesting that neural systems exhibit optimal computational properties at criticality [10–12] further support the criticality hypothesis.

However, which mechanisms could drive such complex systems toward a critical state? Ideally, criticality is reached by a decentralized, self-organized mechanism, an idea known as self-organized criticality (SOC) [13–15]. Models for self-organized criticality in neural networks were discussed even before experimental indications of neural criticality [5], including a self-organized critical adaptive network model [3,16], as well as an adaptation of the Olami-Feder-Christensen SOC model for earthquakes [17] in the context of neural networks [18].

The seminal paper of Beggs and Plenz [5] eventually inspired a multitude of self-organized critical neural network models, often with a particular focus on biological details in the self-organizing mechanisms. Some of these mechanisms are based on short-term synaptic plasticity [19], spike timing dependent plasticity [20], long-term plasticity [21], while others rely on Hebbian-like rules [22–24] or anti-Hebbian rules

[25]. For recent reviews on criticality in neural systems see Refs. [26–31].

In this paper we revisit the earliest model, the self-organized critical adaptive network [3], in the wake of the observation of neural avalanches and ask two questions: Does this general model still self-organize to criticality when adapted to the particular properties of neural networks? How do its avalanche statistics compare to experimental data? Our aim remains to formulate the simplest possible model, namely, an autonomous dynamical system that generates avalanche statistics without external parameters and without any parameter tuning.

The original SOC network model [3] had been formulated as a spin system in the tradition of statistical physics, with binary nodes of values $\sigma \in \{-1, 1\}$, corresponding to inactive and active states respectively. To study avalanches in the critical state, a translation to Boolean state nodes $\sigma(t) \in \{0, 1\}$ is necessary, as has been formulated for modeling biological networks in Ref. [32]. For an adaptive neural network model with rewiring based on the correlation between neighboring nodes [16], we demonstrated earlier that in such a binary realization, avalanche statistics become accessible and exhibit self-organized criticality [33]. Nevertheless, the correlation-based rewiring of that model is not the simplest possible rule, and its algorithmic implementation falls short of a fully autonomous dynamical system: Its adaptation rule still uses data from different simulation runs to determine the synaptic change to be performed.

Therefore, we here reconsider the simpler activity-based rewiring and reformulate our model as a fully autonomous system with adaptation dynamics based on solely local information. It uses Boolean state nodes on a network without a predefined topology. The network topology changes by link adaptations (addition and removal of links) based on local

----
[*]bornholdt@itp.uni-bremen.de

information only, namely, the temporally averaged activity of single nodes. Neither information of the global state of the system nor information about neighboring nodes, e.g., activity correlations [33] or retrosynaptic signals [21], are needed. Last, it is well motivated by abundant evidence for homeostatic processes in neural plasticity.

II. THE MODEL

Let us now define our model in detail. Consider a directed graph with N nodes with binary states $\sigma(t) \in \{0, 1\}$ representing resting and firing nodes. Signals are transmitted between nodes i and j via activating or inhibiting links $c_{ij} \in \{-1, 1\}$. If there is no connection between i and j, then we set $c_{ij} = 0$. Besides the fast dynamical variables $\sigma(t)$ of the network, the connections c_{ij} form a second set of dynamical variables of the system which are evolving on a considerably slower timescale than the node states $\sigma(t)$. Let us define these two dynamical processes, activity dynamics and network evolution, separately.

A. Activity dynamics

The state $\sigma_i(t + \Delta t)$ of node i depends on the input

$$f_i(t) = \sum_{j=1}^{N} c_{ij} \sigma_j(t) \tag{1}$$

at some earlier time t. For simplicity of simulation we here choose a time step of $\Delta t = 1$ and perform parallel update such that this time step corresponds to one sweep where each node is updated exactly once. Please note that random sequential update as well as an autonomous update of each node according to a given internal timescale is possible as well and does not change our results. Having received the input $f_i(t)$, node i will be active at $t + 1$ with a probability

$$\text{Prob}[\sigma_i(t + 1) = 1] = \frac{1}{1 + \exp[-2\beta(f_i(t) - 0.5)]}. \tag{2}$$

Here, β is an inverse temperature, solely serving the purpose of quantifying the amount of noise in the model. For the low-temperature limit $\beta \to \infty$ the probability Eq. (2) becomes a step function which equals 0 for $f_i < 0.5$ and 1 for $f_i > 0.5$. This function broadens for decreasing β, also allowing for nodes being active once in a while without receiving any input. Such idling activity is observed in cortical tissue and will play a role in the evolutionary dynamics as defined in the following.

This model attempts to formulate the simplest rules for the activity dynamics possible, i.e., with the fewest states of the nodes and the fewest parameters. Thus the dynamics neither consider a refractory time nor a nonzero activation threshold. Nevertheless, as shown in Sec. V, the mechanism driving the network toward criticality works in very different biologically inspired implementations of the model. This suggests that despite being a coarse simplification of a real biological system, the model can represent basic mechanisms that can also be at work in real neuronal systems.

B. Network evolution

Following the natural timescale separation between fast neuron dynamics and slow change of their connectivity, we here implement changes of the network structure itself on a well-separated slow timescale. For every time step, each node is chosen with a small probability $\frac{\mu}{N} \ll 1$ and its connectivity is changed based on its average activity $A_i = \langle \sigma_i \rangle_W$ over the time window of the last W time steps according to the following rules:

(i) $A_i = 0$: add a new incoming link $c_{ij} = 1$ from another randomly chosen node j.

(ii) $A_i = 1$: add a new incoming link $c_{ij} = -1$ from another randomly chosen node j.

(iii) $A_i \notin \{0, 1\}$: remove one incoming link of node i.

Thus, inactive (i.e., nonswitching) nodes receive new links, while active (i.e., switching) nodes lose links. These rules prevent the system from reaching, both, an ordered phase where all nodes are permanently frozen, as well as a chaotic regime with abundant switching activity. In particular, the system is driven toward a dynamical phase transition between a globally ordered and a globally chaotic phase.

Note that rewiring is based on locally available information only. To simulate the way a single cell could keep a running average, we also implemented the average activity of a node as $A_i(t + 1) = \sigma(t + 1)(1 - \alpha) + A_i(t)\alpha$ as the basic principle, a biochemical average would be taken. Here, the parameter $\alpha \in [0, 1]$ determines the temporal memory of the nodes (instead of the averaging time window parameter W). Since the newly defined A_i can only approach but never attain 0 or 1, we have to reformulate the criteria which determine the type of rewiring to be performed. The condition for a node to receive an activating link is transformed from $A_i = 0$ to $A_i < \epsilon$ with $\epsilon \ll 1$, the other criteria are changed correspondingly. Then, we find that the model works accordingly.

For practical purposes, we perform the rewiring of only one randomly chosen node i after every $\frac{N}{\mu}$ sweeps, instead of selecting every node with a certain probability $\frac{\mu}{N}$ at each time step. Both implementations yield the same results. To minimize the number of model parameters, we quantify the separation between fast and slow timescales in the model with one parameter by setting $\frac{N}{\mu} = W$ and using W as the parameter.

The proposed rules for the network evolution are inspired by synaptic wiring and rewiring as observed in early developmental stages of neural populations or during the rewiring of dissociated cortical cultures [34]. In these systems, homeostatic plasticity mechanisms are at work, which lead to increased activity of overly inactive neurons and vice versa. In Ref. [35] it was found that the application of inhibitory neurotransmitters to pyramidal neurons in isolated cell cultures, and thus a decrease of activity, leads to an increased outgrowth of neurites. In contrast, if excitatory neurotransmitters are applied, a degeneration of dendritic structures is induced [35–37]. These observations were confirmed in experiments where electrical stimulation of neurons showed to inhibit dendritic outgrowth [38] and blocking of activity resulted in increased growth of dendrites [39,40]. Thus, if a neuron is overly inactive or active, it "grows and retracts its dendrites to find an optimal level of input..." [41], which is
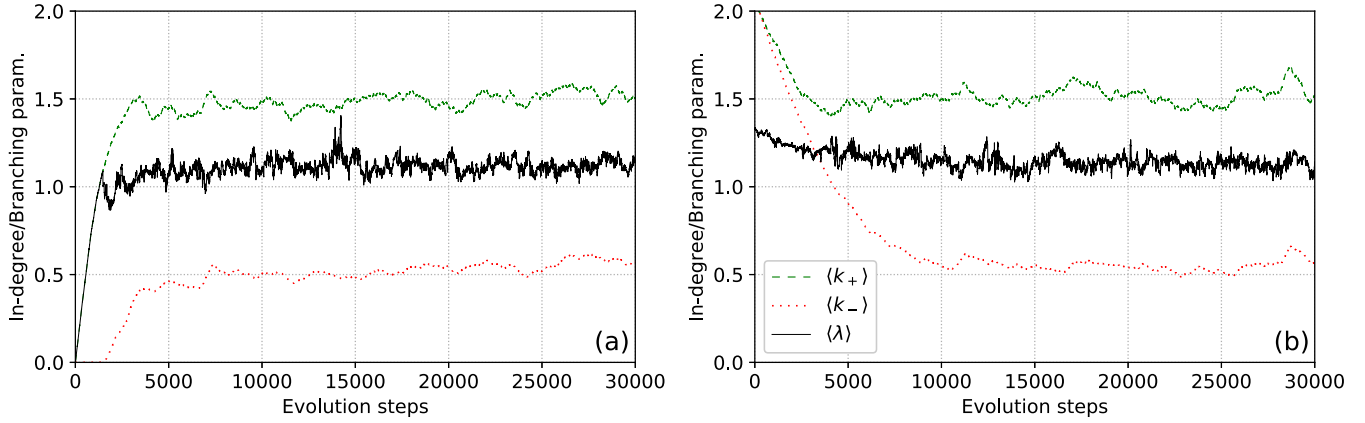
FIG. 1. (a) Time series of the average in-connectivities and branching parameter for $N = 1000$, $\beta = 10$, $W = 1000$, starting from a completely unconnected network. After a transient period, the average connectivities and the branching parameter become stationary. The branching parameter fluctuates around $\langle \lambda \rangle = 1.10 \pm 0.11$, indicating possible criticality. (b) Evolution starts with an average connectivity of $\langle k \rangle = 2$ for activating and inhibiting links. Even though having a very different initial configuration, the system evolves toward a similar steady state as found in panel (a).

mimicked by the proposed rewiring rules. Similar homeostatic adaption rules have been successfully used to model cortical rewiring after deafferentation [42]. In recent models, homeostatic regulation has been proposed as a key mechanism of self-organization and modulation of neural dynamics [43,44].

III. EVOLUTION OF THE NETWORK STRUCTURE

The evolution of the network starts with a specified initial configuration of links $\mathbf{c}(t = 0)$ and the state of all nodes set to $\boldsymbol{\sigma}(t = 0) = \mathbf{0}$. Doing so, all activity originates from small perturbations caused by stochastic noise. Applying the rewiring rules, the system then evolves toward a dynamical steady state with characteristic average numbers of activating and inhibiting links.

As a convenient observable of the dynamical state of the network, and an approximate indicator of a possible critical state of the network, we measure the branching parameter $\langle \lambda \rangle$ by calculating, for every node i, how many neighbor nodes λ on average change their state at time $t + 1$ if the state of i is changed at time t. Averaging λ over the network indicates the dynamical regime of the network, where $\langle \lambda \rangle = 1$ is often used as an indicator of criticality. Note that, by construction, $\langle \lambda \rangle$ depends on the connectivity matrix $c_{ij}(t)$ and on the state vector $\boldsymbol{\sigma}(t)$ and, therefore, has to be considered with some caution. For example, its critical value may differ from one when the evolved networks develop community structure or degree correlations between in- and out-links or between nodes [10]. Therefore, we will here use the branching parameter for a qualitative assessment of the network evolution, only, and analyze criticality with tools from dynamical scaling theory below.

Let us now turn to the evolutionary dynamics of the model, starting from a random network $\mathbf{c}(t = 0)$ with only the average connectivity specified at $t = 0$. Figure 1(a) shows the time series of the average number of incoming activating and inhibiting links per node $\langle k_+ \rangle$ and $\langle k_- \rangle$ starting from a fully unconnected network. The figure also shows the temporal

evolution of the branching parameter $\langle \lambda \rangle$. At the beginning of the network evolution, there are only a few links between the nodes, and noise-induced activity dies out fast. Therefore, the activity is very low, and only activating links are added. As a result, the branching parameter increases. When the value of $\langle k_+ \rangle$ approaches one, the activity starts to propagate through the network and some nodes become permanently active. This causes the rewiring algorithm to insert inhibiting links. After some transient time, the average connectivities become stationary and fluctuate around a mean value. The branching parameter also becomes stationary and fluctuates around a value near one, indicating a possible critical behavior. The ratio of inhibiting links to activating links approximately attains $\langle k_- \rangle / \langle k_+ \rangle \approx 0.3$ which is close to the ratio of inhibition/activation typically observed in real neural systems [45]. The connectivity in the stationary states exhibits Poisson-distributed degree distributions of incoming and outgoing links.

Figure 1(b) shows the evolution of the average connectivities with different initial conditions. Here, the initial average connectivities are chosen as $\langle k_+ \rangle = \langle k_- \rangle = 2$. In contrast to the starting configuration in Fig. 1(a), the network is densely connected and the nodes change their states often. Since the nodes rarely stay in the same state during the averaging time W, links are preferentially deleted in the beginning. After a transient period, the system reaches a stationary steady state similar to the one already observed in Fig. 1(a), indicating independence from initial conditions.

This scenario is reminiscent of synaptic pruning during adolescence, where in some regions of the brain approximately 50% of synaptic connections are lost [46]. It is hypothesized that this process contributes to the observed increase in efficiency of the brain during adolescence [47]. In the proposed model, starting with the densely connected network shown in Fig. 1(b), the branching parameter is considerably larger than one. In this state, information transmission and processing are difficult since already small perturbations percolate through the entire network. The
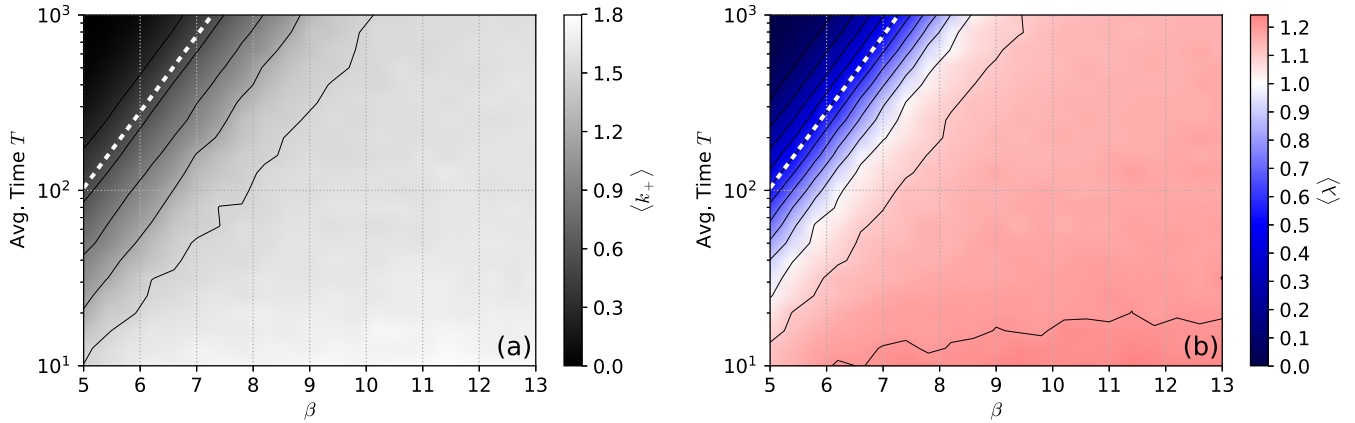
FIG. 2. (a) The average connectivity of activating incoming links $\langle k_+ \rangle$ for different values of the averaging length W and the inverse temperature β. The white dotted line is the upper bound of W given by Eq. (4). (b) The average branching parameter $\langle \lambda \rangle$ for different values of the averaging window length W and the inverse temperature β. The average branching parameter is close to a typical value near one over a broad range of (β, W). The data was obtained by averaging over 30 000 evolution steps, system size is $N = 1000$.

decrease in the number of links leads to a network with a branching parameter close to one, much better suited for information processing tasks.

To explore the parameter dependency of the model, let us now ask how the steady-state averages of the connectivities and the branching parameter depend on the system parameters (β, W, N). Figure 2(a) shows the average connectivity of activating incoming links over a broad range of parameter space. A prominent feature is the subcritical region (upper left corner) where the algorithm fails to create connected graphs and the average connectivity of incoming links is far below one. This is due to nodes being predominantly active by noise, instead of signal transmission. If a node i has no incoming links its probability to be turned on at least once by noise during the W time steps is given by

$$\text{Prob}(A_i > 0) = 1 - \left(1 - \frac{1}{1 + e^\beta} \right)^W. \quad (3)$$

Therefore, demanding that on average not more than half of the nodes should be turned on by noise during W steps gives an upper bound for the time window W:

$$W_{\max} = -\frac{\log 2}{\log \left(1 - \frac{1}{1 + e^\beta} \right)}. \quad (4)$$

This boundary is shown as a white dashed line in Fig. 2(a), obviously being a good approximation for the boundary of the subcritical region. Most importantly, we see that if β is sufficiently large, i.e., if the noise is sufficiently small, then there always is a region in which connected networks emerge. Since $W_{\max}$ is independent of system size N, this also holds for large systems. Figure 2(b) shows the average branching parameter for the same range of (β, W) as Fig. 2(a). Note that $\langle \lambda \rangle$ is close to a value slightly larger than one, over a wide range of noise and averaging times. To explore whether this indicates criticality (with a critical branching parameter value larger than one for the evolved networks), let us now explore other criteria of criticality.

IV. CRITICALITY

An important feature of critical systems is scale-independent behavior, meaning that close to a phase transition similar patterns can be observed on all scales. Near criticality, correlations between distant parts of the system do not vanish and microscopic perturbations can cause influences on all scales. This also implies that power laws occur in many observables, as, e.g., in the size distribution of fluctuations.

A. Avalanches of perturbation spreading

Let us now investigate the statistics of avalanches of perturbations spreading on the networks. Note that the network evolution drives the system toward a state where activity never dies out. Therefore, we cannot consider avalanches of activity-spreading, as usually done in numerical experiments, with one perturbation at a time. The problem of persistent activity could be circumvented by introducing an activity threshold that defines the start and the end of avalanches as done in Ref. [48]. This procedure, nevertheless, is not reliable since the introduction of an activity threshold can generate power-law-like scaling from uncorrelated stochastic processes as was shown in Ref. [49]. Instead, showing that the size and duration of the fluctuations are power-law distributed is a more reliable procedure commonly used in statistical physics [50]. This method is related to the determination of the Boolean Lyapunov exponent, which was used, e.g., in Ref. [51] to examine the critical behavior of neural networks.

First, we let the system evolve until the branching parameter and the average connectivities reach steady average values. Then, noise is deactivated and a copy $\boldsymbol{\sigma}_c$ of the network is made. One node of this copy is chosen at random and its state is flipped: If it was active, then it is turned inactive and vice versa. By comparing the temporal evolution of the unperturbed system $\boldsymbol{\sigma}$ and the perturbed system $\boldsymbol{\sigma}_c$ one can examine the spreading of this perturbation. For quantifying the "difference" between the two copies it is convenient to use the Hamming distance of the state vectors $d_H(\boldsymbol{\sigma}, \boldsymbol{\sigma}_c)$ which is defined as the number of differing entries in $\boldsymbol{\sigma}$ and $\boldsymbol{\sigma}_c$,
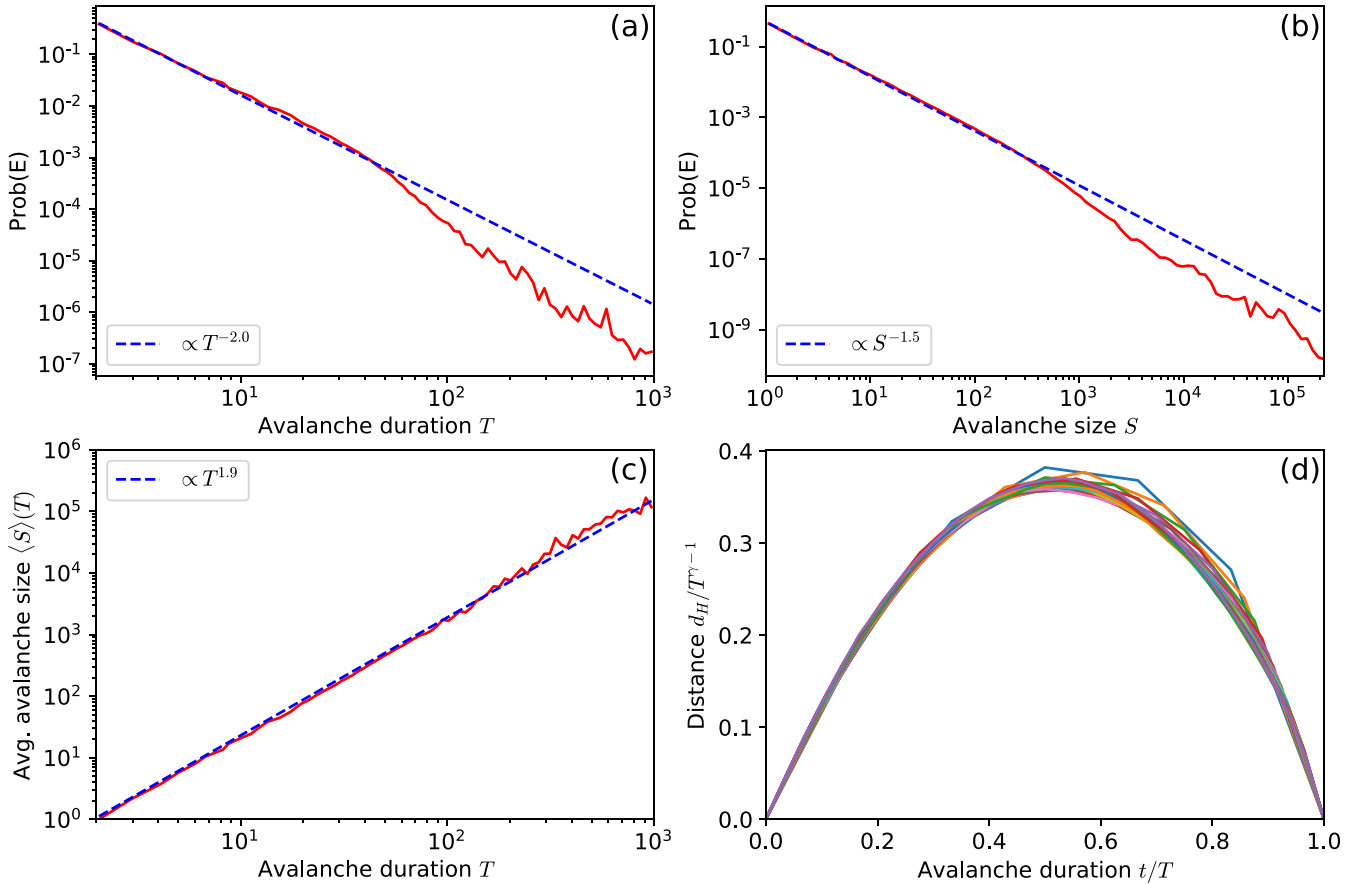
FIG. 3. Avalanche statistics and collapse of avalanche profiles. (a) Avalanche duration distribution. (b) Avalanche size distribution. (c) Average avalanche size over avalanche duration. (d) Collapse of avalanche shapes. The curves show the Hamming distance during avalanches of lengths between 5 and 30. $N = 2000$, $W = 1000$, $\beta = 10$, data from 6×10^6 avalanches.

i.e., the number of nodes which deviate from each other in their states. During the examination of one perturbation, the rewiring algorithm is not in action.

Performing simulations we found that in most cases $d_H(\sigma, \sigma_c) \to 0$ after some time, which means that the perturbed system falls back onto the attractor of the unperturbed system. For a system of, e.g., 2000 nodes with $\beta = 10$ and $W = 1000$, this was observed in more than 90% of all perturbations.

It is straightforward to define the avalanche duration T as the time between the start of the perturbation and the return of σ_c to the same attractor as σ and the avalanche size S as the cumulative sum of the Hamming distances between σ and σ_c during the avalanche:

$$S = \sum_{t=0}^{T} d_H[\sigma(t), \sigma_c(t)]. \quad (5)$$

From universal scaling theory [52] it is expected that these observables exhibit power-law scaling at criticality:

$$\text{Prob}(S) \sim S^{-\tau}, \quad (6)$$

$$\text{Prob}(T) \sim T^{-\alpha}. \quad (7)$$

Furthermore, it should also hold that the relation between the average avalanche size and the avalanche duration shows

power-law scaling

$$\langle S \rangle(T) \sim T^{-\gamma}, \quad (8)$$

with the exponents fulfilling the relation

$$\frac{\alpha - 1}{\tau - 1} = \gamma. \quad (9)$$

To further verify criticality it is possible to explicitly show the scale-freeness of the avalanche dynamics. This can be done by determining the average avalanche profiles (avalanche size over time) for different avalanche durations. Scaled properly, these shapes should collapse onto one universal curve if the system is critical.

B. Results

Figure 3 shows the distribution of avalanche sizes and durations as well as the collapse of avalanche profiles for avalanches of different durations. Exponents were fitted using the estimator for discrete integer variables described in Ref. [53].

Figure 3(a) shows that the avalanche duration scales with an exponent of $\alpha \approx 2.0332 \pm 0.0004$ up to the square root of the system size.

Figure 3(b) reveals a power-law scaling of the avalanche size with an exponent of $\tau \approx 1.5428 \pm 0.0002$. Both
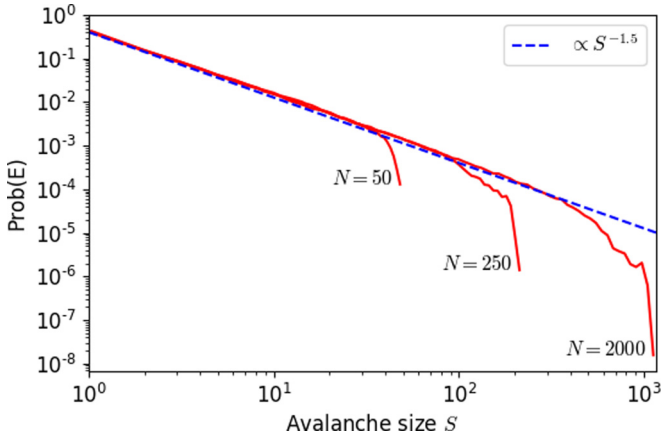
FIG. 4. Scaling of the avalanche size distribution with increasing system size N. Each distribution is obtained from 10^6 avalanches. During one avalanche each node can only contribute once to the avalanche size. Parameters: $\beta = 10, W = 1000$.

exponents α and τ are in line with experimental results [5,8]. Note that the right end of the avalanche duration and size distributions underestimates the true numbers of avalanches, as we here only count avalanches that return to the same attractor as in the unperturbed network. Larger avalanches more frequently end up in a different attractor when perturbed, resulting in a larger fraction of long avalanches not counted in the statistic.

Figure 3(c) shows that the relation between average avalanche size and avalanche duration also exhibits a power-law scaling up to the square root of system size with an exponent of $\gamma \approx 1.92 \pm 0.04$. These exponents fulfill the relation

$$\frac{\alpha - 1}{\tau - 1} = 1.9036 \pm 0.0003 \approx \gamma, \qquad (10)$$

strongly suggesting that the system is critical.

Figure 3(d) shows the collapse of the activity curves onto one universal shape, as it was also found in experiments [8], reflecting the fractal structure of the avalanche dynamics.

A further verification of criticality can be found in Fig. 4, which shows the avalanche size distributions for different systems sizes N. Figure 4 uses a different definition of avalanche size than previously introduced. Here, instead of the sum of Hamming distances between perturbed and unperturbed networks, the avalanche size is the number of nodes that, at any time, have had a different state in the perturbed and the unperturbed network, where every node can only contribute once to the avalanche size. This means that the maximum avalanche size is N. With increasing system size the power-law-like regions of the distributions increase, showing that the cut-off is only a finite size effect.

V. OTHER VERSIONS OF THE MODEL

The main goal of this work is to present a minimal adaptive network model that exhibits self-organized critical behavior. At the same time, the model is supposed to be plausible, in the sense that only local information is used to approach the critical state. While we simulate this model on a von Neumann computer, a fully autonomous implementation is possible. To further demonstrate that our model represents a general mechanism and does not depend on particular features of the implementation, also variants of the model were tested.

A. Inhibiting nodes

We tested a variant that uses inhibiting nodes instead of inhibiting links (and excitatory nodes instead of excitatory links). In this modified model, nodes are connected by un-weighted links and the sign of the outgoing signal is determined by the nature of the node. Before starting the evolution of the network a fraction of all nodes is chosen to be inhibitory. Here we typically choose 20–30%, as it is often used as a rough approximation for real neural systems [45] (simulations show that in the frame of the model the exact number is not of importance). If an inhibitory node is active, it contributes a signal -1 to the inputs of all nodes to which it is connected via outgoing links, and vice versa for excitatory nodes. Further, the network evolution rules of our model are rewritten accordingly and now take the simple form:

(i) $A_i = 0$: add a new incoming link from another randomly chosen excitatory node j.

(ii) $A_i = 1$: add a new incoming link from another randomly chosen inhibitory node j.

(iii) $A_i \notin \{0, 1\}$: remove one incoming link of node i.

We find that the dynamics of this modified version closely resembles the dynamics of the original model.

B. Continuous link weights

Choosing discrete link weights $c_{ij} \in \{-1, 0, 1\}$ allows for a minimalistic description of the model and to formulate simple rules for the network evolution. However, to mimic the varying synaptic strengths of a real neural system, a version with continuous link weights has also been examined. We find that the following continuous rewiring rules lead to critical behavior, as well. In the same way as in the original model, after every W time steps, one node i is chosen at random. Depending on its average activity A_i its linkage is changed as described in the following:

(i) $A_i = 0$: randomly choose another node j. If $c_{ij} = 0$, then add a new incoming link $c_{ij} \in [0, \Delta]$. If $c_{ij} \neq 0$ multiply the link weight by a factor $[1 + \delta \operatorname{sign}(c_{ij})]$.

(ii) $A_i = 1$: randomly choose another node j. If $c_{ij} = 0$, then add a new incoming link $c_{ij} \in [-\Delta, 0]$. If $c_{ij} \neq 0$ multiply the link weight by a factor $[1 - \delta \operatorname{sign}(c_{ij})]$.

(iii) $A_i \notin \{0, 1\}$: randomly choose one incoming link of i. If $|c_{ij}| < 1$, then set $c_{ij} = 0$; otherwise, decrease the link weight by a factor $(1 - \delta)$.

Hereby, the additional parameters δ and Δ should be chosen such that $\delta \ll 1$ to keep incremental changes small, and $\Delta > 2$ for new links to have a dynamical effect in the face of the threshold update rule. Then the network robustly reaches a critical state.

VI. CONCLUSION AND OUTLOOK

In this article, we tried to sketch the simplest possible neural network model that self-organizes toward a critical state,

while reproducing detailed features of criticality observed in real biological neural systems.

Note that the model involves only three parameters, none of which is critical: The inverse temperature β determining the amount of noise in the model, the averaging time W defining the timescale separation between the fast neural dynamics and the slow homeostatic plasticity, and the system size N. None of these needs fine-tuning and they can be varied over a considerable range.

The homeostatic evolution of the network connectivity is based on the temporally averaged activity of single nodes only. Thus, neither information about the global state of the network, nor information about neighboring nodes is necessary for self-organized criticality in this neural network. The model is a variation of the earlier spin-based network SOC model [3], in an implementation with neurons with states zero and one, with a stochastic update rule, allowing for spontaneous activity, and with an evolution rule that specifies inhibitory and excitatory links separately.

Theoretical studies have demonstrated that neural networks can be tuned to criticality by properly adjusting the ratio of activating and inhibiting nodes/links [48]. This is in line with experimental results, which indicate that critical behavior arises in cortical networks with a balanced activation/inhibition ratio [11,54]. In the model studied here, we observe that the balance of inhibitory and excitatory links self-organizes to a steady state. It is possible that mechanisms of similar form help to keep the balance between activation and inhibition especially during early developmental stages of neural systems [34] where phases of rapid synaptic production [46] and synaptic pruning occur [47].

In contrast to the classical models of self-organized criticality, as, e.g., the sandpile model [13], the Bak-Sneppen model of evolution [15], or the forest fire model [14], the model we study here exhibits critical dynamics over a broad range of noise. Indeed, it even utilizes noise to sustain activity

permanently. The origin of the noise resilience of this class of, what we could call "robust self-organized criticality" models, is the fact that the criticality of the system is stored in separate variables, in our case in the links between the nodes, rather than in the dynamical variables, the node states, themselves. Classical SOC models, on the other hand, are more vulnerable against noise as can be seen, for example, in the forest fire model, where criticality emerges as a fractal distribution of tree states that is easily disturbed. In our self-organized critical adaptive network model, in contrast, noise may vary over a broad range.

We have further explored the robustness of the rewiring mechanism in different versions of the model where, for example, inhibiting nodes instead of inhibiting links are implemented or continuous link weights are used. This illustrates that the observed self-organized critical characteristics arise as stable phenomena independent of even major features of the system, only depending on the structure of the rewiring algorithm. Together with the robustness against noise, these observations give strong support to the hypothesis that also real biological neural systems could take advantage of this simple and robust way to self-tune close to a phase transition.

Future work on minimal neural network models showing self-organized critical behavior could focus on how criticality influences learning, as it already has been touched on, e.g., in Refs. [21,24]. Further insights into this field could not only help our understanding of biological neural systems but also motivate new ways of constructing artificial neural networks optimally. The autonomous nature of the self-organized critical adaptive neural network should make it implementable with memristors or other forms of neuromorphic hardware.

[1] C. G. Langton, Computation at the edge of chaos: Phase transitions and emergent computation, Physica D: Nonlin. Phenom. **42**, 12 (1990).

[2] A. V. Herz and J. J. Hopfield, Earthquake Cycles and Neural Reverberations: Collective Oscillations in Systems with Pulse-Coupled Threshold Elements, Phys. Rev. Lett. **75**, 1222 (1995).

[3] S. Bornholdt and T. Rohlf, Topological Evolution of Dynamical Networks: Global Criticality from Local Dynamics, Phys. Rev. Lett. **84**, 6114 (2000).

[4] P. Bak and D. R. Chialvo, Adaptive learning by extremal dynamics and negative feedback, Phys. Rev. E **63**, 031912 (2001).

[5] J. M. Beggs and D. Plenz, Neuronal avalanches in neocortical circuits, J. Neurosci. **23**, 11167 (2003).

[6] J. M. Beggs and D. Plenz, Neuronal avalanches are diverse and precise activity patterns that are stable for many hours in cortical slice cultures, J. Neurosci. **24**, 5216 (2004).

[7] T. Petermann, T. C. Thiagarajan, M. A. Lebedev, M. A. Nicolelis, D. R. Chialvo, and D. Plenz, Spontaneous cortical activity in awake monkeys composed of neuronal avalanches, Proc. Natl. Acad. Sci. U.S.A. **106**, 15921 (2009).

[8] N. Friedman, S. Ito, B. A. Brinkman, M. Shimono, R. L. DeVille, K. A. Dahmen, J. M. Beggs, and T. C. Butler, Universal Critical Dynamics in High Resolution Neuronal Avalanche Data, Phys. Rev. Lett. **108**, 208102 (2012).

[9] W. L. Shew, W. P. Clawson, J. Pobst, Y. Karimipanah, N. C. Wright, and R. Wessel, Adaptation to sensory input tunes visual cortex to criticality, Nat. Phys. **11**, 659 (2015).

[10] D. B. Larremore, W. L. Shew, and J. G. Restrepo, Predicting Criticality and Dynamic Range in Complex Networks: Effects of Topology, Phys. Rev. Lett. **106**, 058101 (2011).

[11] W. L. Shew, H. Yang, S. Yu, R. Roy, and D. Plenz, Information capacity and transmission are maximized in balanced cortical networks with neuronal avalanches, J. Neurosci. **31**, 55 (2011).

[12] W. L. Shew, H. Yang, T. Petermann, R. Roy, and D. Plenz, Neuronal avalanches imply maximum dynamic range in cortical networks at criticality, J. Neurosci. **29**, 15595 (2009).

[13] P. Bak, C. Tang, and K. Wiesenfeld, Self-organized criticality, Phys. Rev. A **38**, 364 (1988).

[14] B. Drossel and F. Schwabl, Self-Organized Critical Forest-Fire Model, Phys. Rev. Lett. **69**, 1629 (1992).

[15] P. Bak and K. Sneppen, Punctuated Equilibrium and Criticality in a Simple Model of Evolution, Phys. Rev. Lett. **71**, 4083 (1993).

[16] S. Bornholdt and T. Röhl, Self-organized critical neural networks, Phys. Rev. E **67**, 066118 (2003).

[17] Z. Olami, Hans Jacob S. Feder, and K. Christensen, Self-Organized Criticality in a Continuous, Nonconservative Cellular Automaton Modeling Earthquakes, Phys. Rev. Lett. **68**, 1244 (1992).

[18] C. W. Eurich, J. M. Herrmann, and U. A. Ernst, Finite-size effects of avalanche dynamics, Phys. Rev. E **66**, 066137 (2002).

[19] A. Levina, J. M. Herrmann, and T. Geisel, Dynamical synapses causing self-organized criticality in neural networks, Nat. Phys. **3**, 857 (2007).

[20] C. Meisel and T. Gross, Adaptive self-organization in a realistic neural network model, Phys. Rev. E **80**, 061917 (2009).

[21] V. Hernandez-Urbina and J. M. Herrmann, Self-organised criticality via retro-synaptic signals, Front. Phys. **4**, 54 (2017).

[22] L. de Arcangelis, C. Perrone-Capano, and H. J. Herrmann, Self-Organized Criticality Model for Brain Plasticity, Phys. Rev. Lett. **96**, 028107 (2006).

[23] G. L. Pellegrini, L. de Arcangelis, H. J. Herrmann, and C. Perrone-Capano, Activity-dependent neural network model on scale-free networks, Phys. Rev. E **76**, 016107 (2007).

[24] L. de Arcangelis and H. J. Herrmann, Learning as a phenomenon occurring in a critical state, Proc. Natl. Acad. Sci. U.S.A. **107**, 3977 (2010).

[25] M. O. Magnasco, O. Piro, and G. A. Cecchi, Self-Tuned Critical Anti-Hebbian Networks, Phys. Rev. Lett. **102**, 258102 (2009).

[26] W. L. Shew and D. Plenz, The functional benefits of criticality in the cortex, Neuroscientist **19**, 88 (2013).

[27] D. Marković and C. Gros, Power laws and self-organized criticality in theory and nature, Phys. Rep. **536**, 41 (2014).

[28] D. Plenz and E. Niebur, *Criticality in Neural Systems* (Wiley-Blackwell, Hoboken, NJ, 2014).

[29] J. Hesse and T. Gross, Self-organized criticality as a fundamental property of neural systems, Front. Syst. Neurosci. **8**, 166 (2014).

[30] V. Hernandez-Urbina and J. Michael Herrmann, Neuronal avalanches in complex networks, Cogent Phys. **3**, 1150408 (2016).

[31] R. Zeraati, V. Priesemann, and A. Levina, Self-organization toward criticality by synaptic plasticity, arXiv:2010.07888.

[32] M. Rybarsch and S. Bornholdt, Binary threshold networks as a natural null model for biological networks, Phys. Rev. E **86**, 026114 (2012).

[33] M. Rybarsch and S. Bornholdt, Avalanches in self-organized critical neural networks: A Minimal model for the neural SOC universality class, PloS One **9**, e93090 (2014).

[34] Y. Yada, T. Mita, A. Sanada, R. Yano, R. Kanzaki, D. J. Bakkum, A. Hierlemann, and H. Takahashi, Development of neural population activity toward self-organized criticality, Neuroscience **343**, 55 (2017).

[35] M. P. Mattson and S. Kater, Excitatory and inhibitory neurotransmitters in the generation and degeneration of hippocampal neuroarchitecture, Brain Res. **478**, 337 (1989).

[36] M. Mattson, P. Dou, and S. Kater, Outgrowth-regulating actions of glutamate in isolated hippocampal pyramidal neurons, J. Neurosci. **8**, 2087 (1988).

[37] P. Haydon, D. McCobb, and S. Kater, The regulation of neurite outgrowth, growth cone motility, and electrical synaptogenesis by serotonin, Dev. Neurobiol. **18**, 197 (1987).

[38] C. S. Cohan and S. B. Kater, Suppression of neurite elongation and growth cone mentality by electrical activity, Science **232**, 1638 (1986).

[39] R. D. Fields, E. A. Neale, and P. G. Nelson, Effects of patterned electrical activity on neurite outgrowth from mouse sensory neurons, J. Neurosci. **10**, 2950 (1990).

[40] F. Van Huizen and H. Romijn, Tetrodotoxin enhances initial neurite outgrowth from fetal rat cerebral cortex cells in vitro, Brain Res. **408**, 271 (1987).

[41] M. Fauth and C. Tetzlaff, Opposing effects of neuronal activity on structural plasticity, Front. Neuroanat. **10**, 75 (2016).

[42] M. Butz, A. Van Ooyen, and F. Wörgötter, A model for cortical rewiring following deafferentation and focal stroke, Front. Comput. Neurosci. **3**, 10 (2009).

[43] F. Y. Kalle Kossio, S. Goedeke, B. van den Akker, B. Ibarz, and R.-M. Memmesheimer, Growing Critical: Self-Organized Criticality in a Developing Neural System, Phys. Rev. Lett. **121**, 058301 (2018).

[44] J. Zierenberg, J. Wilting, and V. Priesemann, Homeostatic Plasticity and External Input Shape Neural Network Dynamics, Phys. Rev. X **8**, 031018 (2018).

[45] H. Markram, M. Toledo-Rodriguez, Y. Wang, A. Gupta, G. Silberberg, and C. Wu, Interneurons of the neocortical inhibitory system, Nat. Rev. Neurosci. **5**, 793 (2004).

[46] P. Rakic, J.-P. Bourgeois, and P. S. Goldman-Rakic, Synaptic development of the cerebral cortex: Implications for learning, memory, and mental illness, Prog. Brain Res. **102**, 227 (1994).

[47] L. P. Spear, Adolescent neurodevelopment, J. Adolescent Health **52**, S7 (2013).

[48] S.-S. Poil, R. Hardstone, H. D. Mansvelder, and K. Linkenkaer-Hansen, Critical-state dynamics of avalanches and oscillations jointly emerge from balanced excitation/inhibition in neuronal networks, J. Neurosci. **32**, 9817 (2012).

[49] J. Touboul and A. Destexhe, Can power-law scaling and neuronal avalanches arise from stochastic dynamics? PloS One **5**, e8982 (2010).

[50] H. E. Stanley, *Phase Transitions and Critical Phenomena* (Clarendon Press, Oxford, 1971).

[51] C. Haldeman and J. M. Beggs, Critical Branching Captures Activity in Living Neural Networks and Maximizes the Number of Metastable States, Phys. Rev. Lett. **94**, 058101 (2005).

[52] J. P. Sethna, K. A. Dahmen, and C. R. Myers, Crackling noise, Nature **410**, 242 (2001).

[53] A. Clauset, C. R. Shalizi, and M. E. Newman, Power-law distributions in empirical data, SIAM Rev. **51**, 661 (2009).

[54] F. Lombardi, H. Herrmann, C. Perrone-Capano, D. Plenz, and L. De Arcangelis, Balance Between Excitation and Inhibition Controls the Temporal Organization of Neuronal Avalanches, Phys. Rev. Lett. **108**, 228703 (2012).